Solubility and Immunoblot Assay

To examine solubility of mutant myotilin, we used frozen biopsied muscles from human control subjects and from the two myotilinopathy patients, as well as TA muscles of six mice each from the wtMYOT-, mMYOT S60C-, and mMYOT R405K-expressing groups, at 14 days after electroporation. The 1.25-mm^3 specimens of muscle were lysed and homogenized in 150 μL of radioimmunoprecipitation assay buffer containing 50 mmol/L Tris-HCl (pH 7.5), 150 mmol/L NaCl, 1 mmol/L EDTA (pH 8.0), 1% Nonidet P-40, 0.5% sodium deoxycholate, 0.1% SDS, and Roche complete protease inhibitor cocktail (Roche Diagnostics). The lysates were incubated at 4°C for 20 minutes with gentle rotation, and then centrifuged at 15,000 × *g* at 4°C for 20 minutes. The supernatants and precipitates were collected, and the protein concentrations of the supernatants were determined using a protein assay kit (Bio-Rad Laboratories, Hercules, CA). Immunoblotting of the supernatant (detergent-soluble) and precipitate (detergent-insoluble) fractions was performed, as described previously.[23] Glyceraldehyde 3-phosphate dehydrogenase (GAPDH) was used as an internal standard. Immunoreactive complexes on the membranes were detected using enhanced chemiluminescence ECL Plus detection reagent (GE Healthcare, Chalfont St Giles, UK). Insolubility index was calculated as the ratio of the quantity of insoluble protein to the total quantity of proteins (the sum of soluble and insoluble proteins).

Immunoprecipitation

The 5-mm^3 specimens of frozen electroporated mouse muscles isolated at 14 days after electroporation were lysed and homogenized in 0.6 mL of radioimmunoprecipitation assay buffer. The lysates were incubated at 4°C for 20 minutes with gentle rotation, and then centrifuged at 15,000 × *g* at 4°C for 20 minutes. The supernatants were collected, and their protein concentrations were adjusted using a protein assay kit (Bio-Rad Laboratories). Immunoprecipitation was performed as described previously,[23] with agarose-conjugated anti-Myc antibody (Santa Cruz Biotechnology).

Statistical Analysis

Differences between wtMYOT-, mMYOT S60C-, and mMYOT R405K-expressing mice were analyzed with GraphPad Prism version 5 (GraphPad Software, La Jolla, CA). Comparisons among groups were performed by one-way analysis of variance with post hoc Tukey's analysis. Data are expressed as means ± SD.

Results

Mutation Screening and Histochemical Analyses of Muscles from Patients

We performed *MYOT* mutation screening in MFM patients and identified two patients with mutations. Patient 1, harboring a *MYOT* c.179C→G (p.S60C) mutation in exon 2, was a 63-year-old woman with a 6-year-long history of slowly progressive limb muscle weakness. Her mother (deceased) had had muscle weakness. The patient had difficulty in climbing stairs without support, and could not walk for long distances. Her serum creatine kinase level was elevated to 734 IU/L (reference, <200 IU/L). A biopsied specimen from the rectus femoris muscle showed marked variation in fiber size, with some necrotic fibers. Clusters of degenerated fibers with abnormal cytoplasmic inclusions were observed; some fibers with rimmed vacuoles were also seen (Figure 1B). Intermyofibrillar networks were markedly disorganized (Figure 1D). Under electron microscopy, electron-dense materials and cytoplasmic amorphous inclusions of various sizes were seen in some fibers (see Supplemental Figure S1 at *http://ajp.amjpathol.org*). Patient 2 was a 57-year-old woman harboring a *MYOT* c.1214G→A (p.R405K) mutation in exon 9. Detailed clinical symptoms have been described previously.[23] In brief, this patient had a 16-year-long history of slowly progressive proximal limb muscle weakness. Her serum creatine kinase level was mildly elevated (385 IU/l). A specimen from the vastus lateralis muscle showed marked variation in fiber size, scattered fibers with internal nuclei, and small angular fibers. Some fibers with rimmed vacuoles were seen (Figure 1C), and intermyofibrillar networks were disorganized (Figure 1E). Immunohistochemical analysis of muscle specimens from both patients revealed scattered fibers with strong immunoreactive accumulations of myotilin (Figure 1, F and G), which costained with polyubiquitin (Figure 1, H and I), α-B crystallin, BAG3, actin, desmin, and filamin C (see Supplemental Figure S2 at *http://ajp.amjpathol.org*).

Mutant Myotilin Does Not Aggregate in Cultured Cells

To examine the aggregation of mutant myotilins in cultured cells, C2C12 murine myoblasts were transfected with Myc-tagged wtMYOT (Myc-wtMYOT) or Myc-tagged mMYOT (Myc-mMYOT S60C or R405K). After 48 hours, immunostaining with anti-Myc antibody and rhodamine-labeled phalloidin revealed that the expressed Myc-wtMYOT, Myc-mMYOT S60C, and Myc-mMYOT R405K did not form abnormal protein aggregations, and they localized at actin stress fibers (Figure 2). Expression of mMYOT did not affect differentiation of C2C12 cells (data not shown).

Accumulation of Myotilin after Electroporation

To investigate the roles of mutant myotilin, we performed *in vivo* electroporation to express Myc-wtMYOT or Myc-mMYOT (S60C or R405K) in mouse TA muscles. At 7 and 14 days after electroporation, Myc-positive granules with diameters >1 μm were observed in Myc-tagged myotilin-expressing myofibers (Figure 3A). Compared with wtMYOT-expressing myofibers, mMYOT-expressing myofi-

Figure 2. Expression of mutant myotilin in cultured cells. Immunofluorescence staining of transfected Myc-wtMYOT (**A**), Myc-mMYOT S60C (**B**), and Myc-mMYOT R405K (**C**) in C2C12 murine myoblasts. Merged images of Myc-tagged myotilin-expressing cells (green) costained for actin stress fibers (red), and nuclear staining with DAPI (blue). C2C12 myoblasts expressing mMYOT S60C (**B**) or R405K (**C**) did not exhibit protein aggregates, and the mutant myotilin colocalized with actin stress fibers similar to wtMYOT (**A**). Scale bar = 20 μm.

bers contained more granular aggregates that were larger in size. At 7 days after electroporation, Myc-positive aggregates of wtMYOT, mMYOT S60C, and mMYOT R405K were observed in 14 ± 5%, 44 ± 7%, and 21 ± 4% of muscle fibers, respectively (Figure 3B). At 14 days after electroporation, the number of the fibers with aggregates increased to 22 ± 4% in wtMYOT, 50 ± 2% in mMYOT S60C, and 37 ± 3% in mMYOT R405K (Figure 3C). The number and size of Myc-positive aggregates in 30 randomly selected Myc-positive muscle fibers were much higher in mMYOT S60C and slightly higher in mMYOT R405K at 14 days after electroporation than at 7 days (see Supplemental Figure S3 at *http://ajp.amjpathol.org*). These data indicate that the expressed mutant myotilins, and mMYOT S60C in particular, are prone to aggregate in skeletal muscles. The amounts of expressed Myc-tagged myotilin proteins were approximately equal, as measured by immunoblotting (Figure 3D).

Myofibril Disorganization and Z-Disk Streaming in Muscles Expressing Mutant Myotilins

To investigate the ultrastructural characteristics of mutant myotilin-electroporated muscles, we performed electron microscopy at 7 and 14 days after electroporation. In Toluidine Blue-stained longitudinal semithin sections, partial disorganization of the Z-disk was observed in both mMYOT S60C-expressing and mMYOT R405K-expressing TA muscles, but not in control or wtMYOT electroporated muscles (data not shown). Electron microscopy also revealed myofibril disorganization with disrupted Z-disk, such as Z-disk streaming and broadening, in mMYOT-expressing muscles (Figure 4, A and D). Variable-sized (1 to 8 μm in diameter) electron-dense material, with electron densities similar to that of the Z-disk, were also seen in mMYOT-expressing mouse muscles (Figure 4, B and E). The inclusions were occasionally associated with autophagic vacuoles (Figure 4, C and F). These ultrastructural findings were commonly observed in both mMYOT S60C- and mMYOT R405K-expressing mouse muscles.

Mutant Myotilin Aggregates Colocalize with Polyubiquitin and Other Z-Disk–Associated Proteins

To compare the protein accumulations in human and mouse muscles, we performed immunohistochemical analysis. At 14 days after electroporation, some cytoplasmic inclusions were observed in mGT-stained sections of mMYOT-expressing muscles (Figure 5, A and B). Immunostaining of serial sections revealed that the inclusions were immunopositive for the Myc tag (Figure 5, A and B). The aggregates of Myc-mMYOT (S60C and R405K) strongly colocalized with polyubiquitin and αB-crystallin. Accumulations of other Z-disk–associated proteins were also observed, including BAG3, actin, desmin, and filamin C (Figure 5). These findings are similar to the observations made in the patients' muscles (Figure 1, F–I; see also Supplemental Figure S2 at *http://ajp.amjpathol.org*). In the electroporated muscles, Myc-wtMYOT aggregates also colocalized with Z-disk–associated proteins, including αB-crystallin, BAG3, actin, desmin, and filamin C (data not shown), whereas only few wtMYOT aggregates were immunopositive for polyubiquitin (Figure 6A).

Mutant Myotilin Proteins Display Marked Detergent Insolubility with Polyubiquitinated Proteins

In the muscle specimens of the two myotilinopathy patients, myotilin aggregates exhibited positive staining for polyubiquitin (Figure 1; see also Supplemental Figure S3 at *http://ajp.amjpathol.org*). Similarly, in electroporated mouse muscles, mMYOT aggregates were positive for polyubiquitin, and polyubiquitin-positive aggregates were more prominently observed in mMYOT S60C-expressing muscles at 14 days after electroporation. On the other hand, only few aggregates of Myc-wtMYOT were positive for polyubiquitin (Figure 6A). This result suggests that mutant myotilin was ubiquitinated or that the expressed mutant myotilin induced the deposition of polyubiquitinated proteins in the muscles of patients and electroporated mice. To characterize these aggregates, we performed a solubility assay. The muscle

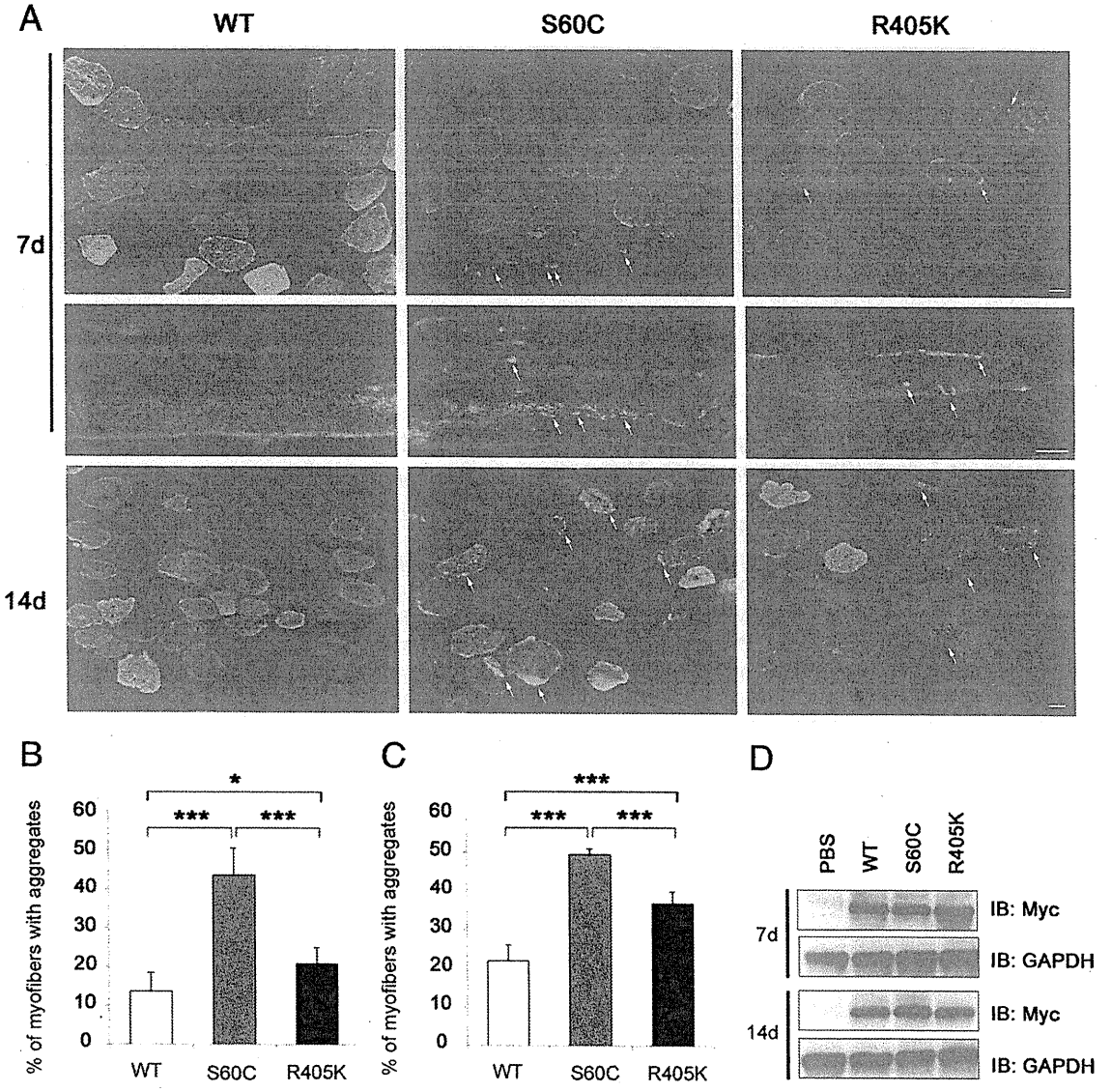

Figure 3. Enhanced aggregation of mutant myotilins in mouse skeletal muscle. **A:** Immunohistochemical staining of Myc-wtMYOT (WT)-electroporated or Myc-mMYOT (S60C or R405K)-electroporated mouse TA muscles. At 7 and 14 days after electroporation, S60C and R405K formed many Myc-positive granular aggregates (**arrows**) in myofibers, compared with WT. More prominent protein aggregates were observed in the S60C-electroporated muscle. At 14 days after electroporation, S60C-expressing myofibers exhibited larger aggregates. Scale bars: 20 μm. **B** and **C:** The percentage of myofibers with Myc-positive aggregates in the electroporated fibers of the WT, S60C, and R405K expression groups (n = 5 mice per group). $^{*}P < 0.05$; $^{***}P < 0.001$. **D:** Immunoblotting analysis of transfected Myc-tagged myotilin in 15 serial sections taken after the sections used for immunohistochemistry. GAPDH was used as a loading control.

specimen with the S60C mutation (patient 1) exhibited increased amounts of myotilin in the detergent-insoluble fraction, compared with the control specimens (Figure 6, B and D). Increasing amounts of polyubiquitinated proteins and αB-crystallin were also detected in the insoluble fraction. On the other hand, the solubilities of myotilin and other proteins, including polyubiquitin, in the muscle specimen with the R405K mutation (patient 2) were similar to those of controls (Figure 6B). Consistently, in the mouse muscles isolated at 14 days after electroporation, markedly increasing amounts of insoluble mMYOT S60C were observed (Figure 6C). In the PBS-injected control muscle, insolubility of endogenous myotilin was 31 ± 12%, whereas in the wtMYOT-, mMYOT S60C-, and mMYOT R405K-injected muscles, the Myc-tagged myotilin amounts in the insoluble fraction were 34 ± 10%, 69 ± 5%, and 48 ± 9%, respectively (Figure 6E). Insolubility of Myc-wtMYOT was similar to that of endogenous myotilin, but mMYOT, and S60C in particular, exhibited higher insolubility (Figure 6E).

These results are consistent with the number of intracellular aggregates observed after electroporation. The amount of polyubiquitinated proteins was markedly increased in the insoluble fraction of mMYOT S60C-electroporated muscles, similar to that of the muscle with the S60C mutation (patient 1) (Figure 6, B and C). A slight increase in the amount of detergent-insoluble polyubiquitinated proteins was observed in mMYOT R405K-electroporated muscles (Figure 6C). The amounts of other

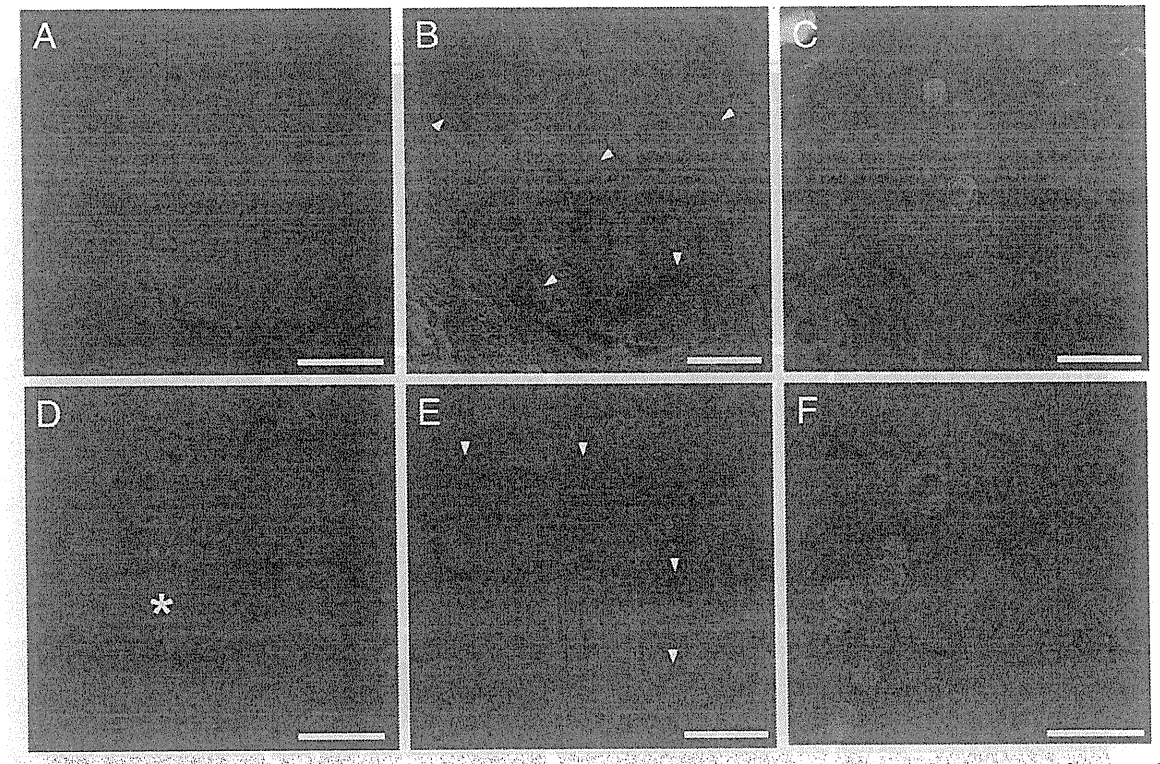

Figure 4. Electron microscopy of muscles expressing mutant myotilin. mMYOT S60C (**A–C**); mMYOT R405K (**D–F**). **A** and **D:** mMYOT-transfected muscle fibers exhibited myofibril disorganization with disrupted Z-disk; note broadening of Z-disks (**A**, **brackets**) and Z-disk streaming (**D**, **asterisk**). **B** and **E:** Variable-sized (1 to 8 μm in diameter) electron-dense inclusions (**arrowheads**) were seen in mMYOT-expressing muscles. **C** and **F:** Inclusions were occasionally associated with autophagic vacuoles (AV). **B** and **C:** Seven days after electroporation. **A** and **D–F:** Fourteen days after electroporation. Scale bars: 3.0 μm (**B** and **E**); 2.0 μm (**C**); 1.7 μm (**A** and **D**); 1.4 μm (**F**).

Z-disk–associated proteins, including αB-crystallin, in the insoluble fraction did not exhibit an increase, even in mMYOT S60C-electroporated muscles (Figure 6C; see also Supplemental Figure S4, A and B, at *http://ajp.amjpathol.org*). We also performed an immunoprecipitation assay to examine whether myotilin was polyubiquitinated. Myc-tagged myotilin proteins were immunoprecipitated from the detergent-soluble fraction of the mouse muscles isolated at 14 days after electroporation. Polyubiquitin immunoreactivity was not detected in the immunoprecipitated proteins (see Supplemental Figure S4C at *http://ajp.amjpathol.org*), indicating that neither the wt-MYOT nor the mMYOT proteins in the soluble fraction were polyubiquitinated.

Discussion

Patients with MFM, including myotilinopathy, exhibit variable clinical features. Some patients exhibit progressive weakness in proximal muscles, whereas others exhibit distal dominant muscle involvement. Cardiomyopathy, peripheral neuropathy, and respiratory insufficiency may be observed.[2] The diagnosis of MFM is generically based on characteristic pathological findings in biopsied muscles, namely, myofibrillar degradation and protein aggregation.[1] Histochemically, the most remarkable pathological changes were observed with mGT staining (Figure 1). Abnormal protein aggregates were observed, including amorphous, granular, or hyaline deposits of various sizes, shapes, and colors (dark blue, blue red, or dark green). The presence of rimmed and nonrimmed vacuoles was also a characteristic observation. Furthermore, NADH-TR staining revealed intermyofibrillar network disorganization. Attenuation or absence of NADH-TR activity in focal areas of myofibers is also observed in MFM.[1,31]

Here, we have presented findings for myotilinopathy patients with similar clinical features but different pathological changes. Fibers with cytoplasmic inclusions and disorganized myofibrils were prominent in the patient with S60C mutation, and these inclusions were strongly immunoreactive for myotilin (Figure 1).

Although transfected cultured cells did not show aggregations, our *in vivo* expression studies in mice were able to reproduce the pathological changes observed in myotilinopathy patients. Mutant myotilin caused enhanced protein aggregation in TA muscles within 1 to 2 weeks (Figure 3). The dark blue or dark green inclusions stained by mGT in mutant-expressing fibers (Figure 4) were similar to those observed in the myotilinopathy patients. Furthermore, mMYOT S60C-expressing myofibers exhibited a greater number of aggregates, which is consistent with the pathology of the patient with that mutation (patient 1). Of note, the size of mMYOT S60C aggregates markedly increased over time, suggesting that mutant myotilin may be resistant to protein degra-

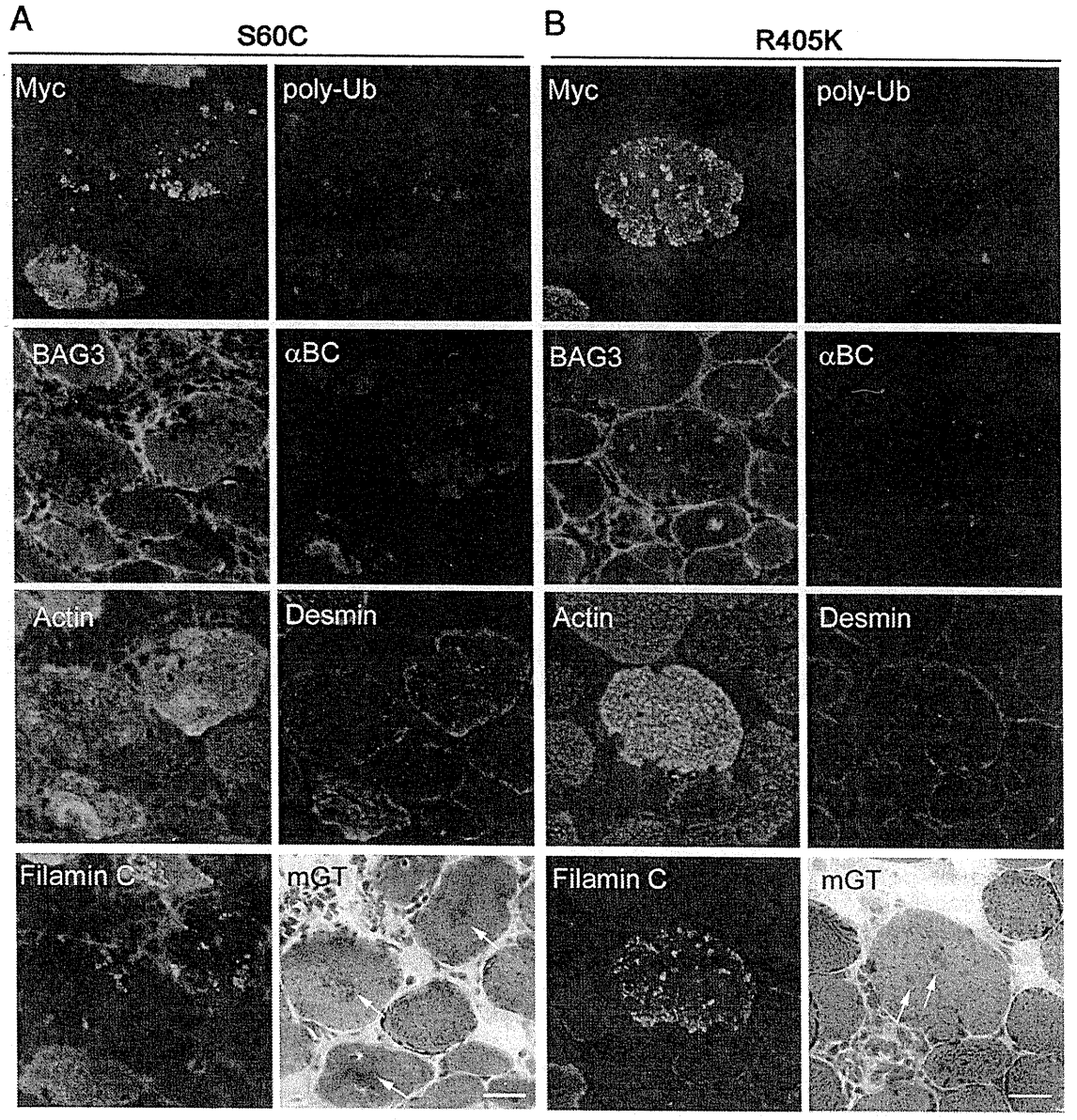

Figure 5. Mutant myotilin aggregates colocalize with polyubiquitin and other Z-disk–associated proteins in electroporated mouse muscle. mGT and immunohistochemical staining of mouse muscle expressing Myc-mMYOT S60C (**A**) or mMYOT R405K (**B**) at 14 days after electroporation. On mGT-stained sections of mMYOT-expressing muscles, cytoplasmic inclusions (**arrows**) were seen. The inclusions were immunopositive for the Myc tag in serial sections. The Myc-positive aggregates of S60C and R405K strongly colocalized with polyubiquitin (poly-Ub) and αB-crystallin (αBC). The aggregates were also immunopositive for BAG3, actin, desmin, and filamin C. Scale bars: 20 μm (**A** and **B**).

dation, as described previously for MFM-associated mutant desmin.[32,33]

Focal disorganization of myofibrils, Z-disk streaming, and accumulation of electron-dense material near the Z-disk are characteristic electron microscopic findings in the muscles of MFM patients.[17,34,35] In the myotilinopathy patient, Z-disk streaming, numerous autophagic vacuoles[17] and cytoplasmic amorphous inclusions were observed (see Supplemental Figure S2 at *http://ajp.amjpathol.org*). In the present study, expression of mMYOT by electroporation elicited myofibril disorganization and accumulation of electron-dense material, which are ultrastructural hallmarks of MFM (Figure 5). Autophagic vacuoles associated with inclusions were also observed in electroporated muscles. Disorganization of myofibrils starting from the Z-disk and material appearing to originate from the Z-disk are commonly observed in MFM patients,[34,35] and these features were also observed in the mMYOT-electroporated muscles. These morphological findings imply that the presence of mutant myotilin can induce characteristic pathological features by affecting Z-disk structure.

Ectopic accumulations of multiple proteins, including Z-disk–associated proteins, are typical pathological features of MFM.[36,37] This study and previous reports[23,38] showed that myotilin-positive protein aggregates colocal-

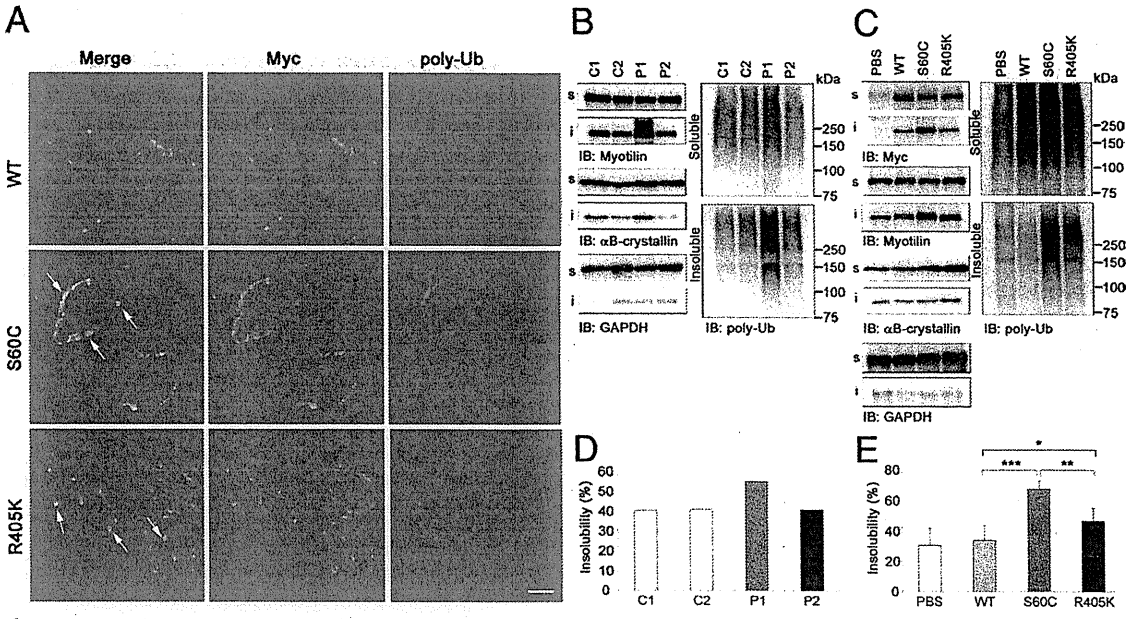

Figure 6. Mutant myotilin displays marked detergent insolubility, along with polyubiquitinated proteins. **A:** At 14 days after electroporation of Myc-wtMYOT (WT) or Myc-mMYOT (S60C or R405K), Myc-mMYOT aggregates, particularly those of S60C, colocalized with polyubiquitin (polyUb) (**arrows**). The WT aggregates rarely costained with polyubiquitin. **B–E** Solubilities of myotilin, polyubiquitinated proteins, and other sarcomeric proteins in muscles from myotilinopathy patients (**B** and **D**) and from electroporated mice (**C** and **E**). GAPDH was used as a loading control. **B:** Immunoblotting of detergent-soluble and detergent-insoluble fractions of muscles from control subjects (C1 and C2) or myotilinopathy patients [P1 (patient 1) and P2 (patient 2)]. In the muscles from P1 with S60C, markedly increasing amounts of myotilin, polyubiquitinated proteins, and αB-crystallin were detected in the insoluble fraction, compared with muscles from control subjects. **D:** Quantification of myotilin insolubilities revealed highest insolubility in P1. **C:** Immunoblotting of detergent-soluble and detergent-insoluble fractions of WT, S60C, or R405K-expressing muscles at 14 days after electroporation. Increasing amounts of insoluble Myc-tagged myotilin proteins and polyubiquitinated proteins were observed in mMYOT-electroporated muscles, compared with WT. Particularly in S60C-electroporated muscles, the amounts of insoluble proteins were notably increased. **E:** Quantification of the insolubilities of electroporated Myc-tagged myotilin in the WT, S60C, and R405K expression groups (n = 6 mice per group). Insolubility of endogenous myotilin was measured using PBS-treated mouse muscles. Compared with WT, insolubilities of electroporated Myc-tagged myotilin were significantly increased in S60C and R405K. $^{*}P < 0.05$; $^{**}P < 0.01$; $^{***}P < 0.001$. Scale bar = 20 μm.

ize with ubiquitin and Z-disk–associated proteins (ie, αB-crystallin, BAG3, actin, desmin, and filamin C) in the muscles of myotilinopathy patients (Figure 1; see also Supplemental Figure S2 at *http://ajp.amjpathol.org*). It has been reported that the myotilin T57I transgenic mice develop progressive myofibrillar changes, including Z-disk streaming and accumulation of mutant myotilin with ubiquitin and Z-disk–associated proteins, similar to those observed in myotilinopathy patients.[28] Expression of mMYOT elicited similar cytoplasmic aggregations in mouse skeletal muscle, and within 2 weeks the aggregates colocalized with polyubiquitin and other Z-disk–associated proteins. Our results indicate that mutant myotilin is able to nucleate aggregations of Z-disk–associated proteins in skeletal muscle.

MFM is a proteinopathy (ie, a protein accumulation disease). In these diseases, protein aggregates are operationally defined by poor solubility in aqueous or detergent solvents.[39,40] Such insoluble protein aggregations are characteristic of many neurodegenerative diseases.[41] In the present study, we discovered that the mutant myotilin S60C protein, along with polyubiquitinated proteins, exhibited marked detergent insolubility in muscles from both the patient and electroporated mice. Mutant myotilin R405K protein showed increased, but lower, detergent insolubility in mice (Figure 6), which may be consistent with the observation that the muscle from the patient with the R405K mutation exhibited only mild protein aggregation (Figure 1). The different detergent insolubilities exhibited by the two *MYOT* mutations may closely correlate with the amounts of protein aggregation. Here, we confirmed the aggregation-prone property of mutant myotilin, which participates in the pathogenesis of myotilinopathy. Using an immunoprecipitation assay, we also showed that electroporated mMYOT was not ubiquitinated in the detergent-soluble fraction (see Supplemental Figure S4 at *http://ajp.amjpathol.org*). A previous study showed that transfected myotilin is degraded by the proteasome system in cultured cells.[42] Our present findings show that ubiquitinated mutant myotilin can form insoluble aggregates. It is also possible that aggregation of insoluble ubiquitinated proteins is induced by the expression of mutant myotilin.

Several causative genes have been identified for MFM; however, in previous studies no mutations were found in nearly half of the MFM patients.[2] To identify the unknown causative genes, easy methods are required for determining the pathogenicity of novel mutations. Some mutant proteins exhibit protein aggregation[43–45] or biological dysfunction, including protein-protein interaction *in vitro*.[23,46–48] However, we could not detect any protein aggregation in mMYOT-expressing cultured cells (Figure 2). The difficulty of *in vitro* investigation may be responsible for the inability to identify Z-disk–associated proteins or mature Z-disk structures. Indeed, myotilin is expressed in later differentiated C2C12 myotubes with

sarcomere-like structures.[49] This suggests that mutant myotilin requires mature Z-disk and/or other sarcomeric proteins to cause aggregations. In such cases, *in vivo* examination is important for evaluating the pathogenicity of mutations. Because *in vivo* electroporation can reproduce the pathological changes observed in MFM patients within a short time, it is a useful and powerful tool for evaluating the pathogenicity of mutations in MFM.

Acknowledgments

We thank Dr. Alan H. Beggs (Children's Hospital Boston, Harvard Medical School) for the kind gift of anti-filamin C antibody and Dr. Satomi Mitsuhashi (Children's Hospital Boston, Harvard Medical School) for technical assistance in electron microscopy analysis.

References

1. Selcen D: Myofibrillar myopathies. Neuromuscul Disord 2011, 21: 161–171
2. Selcen D, Engel AG: Myofibrillar myopathy. (Updated) In GeneReviews. Copyright University of Washington, Seattle. 1997–2012. Available at http://www.ncbi.nlm.nih.gov/books/NBK1499, last revised July 27, 2010
3. OlivÉ M, Odgerel Z, Martínez A, Poza JJ, Bragado FG, Zabalza RJ, Jericó I, Gonzalez-Mera L, Shatunov A, Lee HS, Armstrong J, Maraví E, Arroyo MR, Pascual-Calvet J, Navarro C, Paradas C, Huerta M, Marquez F, Rivas EG, Pou A, Ferrer I, Goldfarb LG: Clinical and myopathological evaluation of early- and late-onset subtypes of myofibrillar myopathy. Neuromuscul Disord 2011, 21:533–542
4. Salmikangas P, Mykkänen OM, Grönholm M, Heiska L, Kere J, Carpén O: Myotilin, a novel sarcomeric protein with two Ig-like domains, is encoded by a candidate gene for limb-girdle muscular dystrophy. Hum Mol Genet 1999, 8:1329–1336
5. Parast MM, Otey CA: Characterization of palladin, a novel protein localized to stress fibers and cell adhesions. J Cell Biol 2000, 150: 643–656
6. Mykkänen OM, Grönholm M, Rönty M, Lalowski M, Salmikangas P, Suila H, Carpén O: Characterization of human palladin, a microfilament-associated protein. Mol Biol Cell 2001, 12:3060–3073
7. Bang ML, Mudry RE, McElhinny AS, Trombitas K, Geach AJ, Yamasaki R, Sorimachi H, Granzier H, Gregorio CC, Labeit S: Myopalladin, a novel 145-kilodalton sarcomeric protein with multiple roles in Z-disc and I-band protein assemblies. J Cell Biol 2001, 153:413–427
8. Faulkner G, Lanfranchi G, Valle G: Telethonin and other new proteins of the Z-disc of skeletal muscle. IUBMB Life 2001, 51:275–282
9. Frank D, Kuhn C, Katus HA, Frey N: The sarcomeric Z-disc: a nodal point in signalling and disease. J Mol Med (Berl) 2006, 84:446–468
10. van der Ven PF, Wiesner S, Salmikangas P, Auerbach D, Himmel M, Kempa S, Hayess K, Pacholsky D, Taivainen A, Schröder R, Carpén O, Fürst DO: Indications for a novel muscular dystrophy pathway. gamma-Filamin, the muscle-specific filamin isoform, interacts with myotilin. J Cell Biol 2000, 151:235–248
11. Gontier Y, Taivainen A, Fontao L, Sonnenberg A, van der Flier A, Carpen O, Faulkner G, Borradori L: The Z-disc proteins myotilin and FATZ-1 interact with each other and are connected to the sarcolemma via muscle-specific filamins. J Cell Sci 2005, 118:3739–3749
12. von Nandelstadh P, Ismail M, Gardin C, Suila H, Zara I, Belgrano A, Valle G, Carpen O, Faulkner G: A class III PDZ binding motif in the myotilin and FATZ families binds enigma family proteins: a common link for Z-disc myopathies. Mol Cell Biol 2009, 29:822–834
13. Witt SH, Granzier H, Witt CC, Labeit S: MURF-1 and MURF-2 target a specific subset of myofibrillar proteins redundantly: towards understanding MURF-dependent muscle ubiquitination. J Mol Biol 2005, 350:713–722
14. Salmikangas P, van der Ven PF, Lalowski M, Taivainen A, Zhao F, Suila H, Schröder R, Lappalainen P, Fürst DO, Carpén O: Myotilin, the limb-girdle muscular dystrophy 1A (LGMD1A) protein, cross-links actin filaments and controls sarcomere assembly. Hum Mol Genet 2003, 12:189–203
15. von Nandelstadh P, Grönholm M, Moza M, Lamberg A, Savilahti H, Carpén O: Actin-organising properties of the muscular dystrophy protein myotilin. Exp Cell Res 2005, 310:131–139
16. Selcen D: Myofibrillar myopathies. Curr Opin Neurol 2008, 21:585–589
17. Olivé M, Goldfarb LG, Shatunov A, Fischer D, Ferrer I: Myotilinopathy: refining the clinical and myopathological phenotype. Brain 2005, 128:2315–2326
18. Foroud T, Pankratz N, Batchman AP, Pauciulo MW, Vidal R, Miravalle L, Goebel HH, Cushman LJ, Azzarelli B, Horak H, Farlow M, Nichols WC: A mutation in myotilin causes spheroid body myopathy. Neurology 2005, 65:1936–1940
19. Hauser MA, Conde CB, Kowaljow V, Zeppa G, Taratuto AL, Torian UM, Vance J, Pericak-Vance MA, Speer MC, Rosa AL: Myotilin mutation found in second pedigree with LGMD1A. Am J Hum Genet 2002, 71:1428–1432
20. Hauser MA, Horrigan SK, Salmikangas P, Torian UM, Viles KD, Dancel R, Tim RW, Taivainen A, Bartoloni L, Gilchrist JM, Stajich JM, Gaskell PC, Gilbert JR, Vance JM, Pericak-Vance MA, Carpen O, Westbrook CA, Speer MC: Myotilin is mutated in limb girdle muscular dystrophy 1A. Hum Mol Genet 2000, 9:2141–2147
21. Penisson-Besnier I, Talvinen K, Dumez C, Vihola A, Dubas F, Fardeau M, Hackman P, Carpen O, Udd B: Myotilinopathy in a family with late onset myopathy. Neuromuscul Disord 2006, 16:427–431
22. Berciano J, Gallardo E, Dominguez-Perles R, Garcia A, Garcia-Barredo R, Combarros O, Infante J, Illa I: Autosomal-dominant distal myopathy with a myotilin S55F mutation: sorting out the phenotype. J Neurol Neurosurg Psychiatry 2008, 79:205–208
23. Shalaby S, Mitsuhashi H, Matsuda C, Minami N, Noguchi S, Nonaka I, Nishino I, Hayashi YK: Defective myotilin homodimerization caused by a novel mutation in MYOT exon 9 in the first Japanese limb girdle muscular dystrophy 1A patient. J Neuropathol Exp Neurol 2009, 68:701–707
24. Reilich P, Krause S, Schramm N, Klutzny U, Bulst S, Zehetmayer B, Schneiderat P, Walter MC, Schoser B, Lochmüller H: A novel mutation in the myotilin gene (MYOT) causes a severe form of limb girdle muscular dystrophy 1A (LGMD1A). J Neurol 2011, 258:1437–1444
25. Mavroidis M, Panagopoulou P, Kostavasili I, Weisleder N, Capetanaki Y: A missense mutation in desmin tail domain linked to human dilated cardiomyopathy promotes cleavage of the head domain and abolishes its Z-disc localization. FASEB J 2008, 22:3318–3327
26. Wang X, Osinska H, Klevitsky R, Gerdes AM, Nieman M, Lorenz J, Hewett T, Robbins J: Expression of R120G-alphaB-crystallin causes aberrant desmin and alphaB-crystallin aggregation and cardiomyopathy in mice. Circ Res 2001, 89:84–91
27. Wang X, Osinska H, Dorn GW 2nd, Nieman M, Lorenz JN, Gerdes AM, Witt S, Kimball T, Gulick J, Robbins J: Mouse model of desmin-related cardiomyopathy. Circulation 2001, 103:2402–2407
28. Garvey SM, Miller SE, Claflin DR, Faulkner JA, Hauser MA: Transgenic mice expressing the myotilin T57I mutation unite the pathology associated with LGMD1A and MFM. Hum Mol Genet 2006, 15:2348–2362
29. Hayashi YK, Matsuda C, Ogawa M, Goto K, Tominaga K, Mitsuhashi S, Park YE, Nonaka I, Hino-Fukuyo N, Haginoya K, Sugano H, Nishino I: Human PTRF mutations cause secondary deficiency of caveolins resulting in muscular dystrophy with generalized lipodystrophy. J Clin Invest 2009, 119:2623–2633
30. Thompson TG, Chan YM, Hack AA, Brosius M, Rajala M, Lidov HG, McNally EM, Watkins S, Kunkel LM: Filamin 2 (FLN2): A muscle-specific sarcoglycan interacting protein. J Cell Biol 2000, 148:115–126
31. Schröder R, Schoser B: Myofibrillar myopathies: a clinical and myopathological guide. Brain Pathol 2009, 19:483–492
32. Liu J, Chen Q, Huang W, Horak KM, Zheng H, Mestril R, Wang X: Impairment of the ubiquitin-proteasome system in desminopathy mouse hearts. FASEB J 2006, 20:362–364
33. Liu J, Tang M, Mestril R, Wang X: Aberrant protein aggregation is essential for a mutant desmin to impair the proteolytic function of the ubiquitin-proteasome system in cardiomyocytes. J Mol Cell Cardiol 2006, 40:451–454
34. Selcen D, Ohno K, Engel AG: Myofibrillar myopathy: clinical, morphological and genetic studies in 63 patients. Brain 2004, 127:439–451

35. Claeys KG, Fardeau M, Schröder R, Suominen T, Tolksdorf K, Behin A, Dubourg O, Eymard B, Maisonobe T, Stojkovic T, Faulkner G, Richard P, Vicart P, Udd B, Voit T, Stoltenburg G: Electron microscopy in myofibrillar myopathies reveals clues to the mutated gene. Neuromuscul Disord 2008, 18:656–666
36. Claeys KG, van der Ven PF, Behin A, Stojkovic T, Eymard B, Dubourg O, Laforêt P, Faulkner G, Richard P, Vicart P, Romero NB, Stoltenburg G, Udd B, Fardeau M, Voit T, Fürst DO: Differential involvement of sarcomeric proteins in myofibrillar myopathies: a morphological and immunohistochemical study. Acta Neuropathol 2009, 117:293–307
37. Olivé M: Extralysosomal protein degradation in myofibrillar myopathies. Brain Pathol 2009, 19:507–515
38. Janué A, Olivé M, Ferrer I: Oxidative stress in desminopathies and myotilinopathies: a link between oxidative damage and abnormal protein aggregation. Brain Pathol 2007, 17:377–388
39. Fink AL: Protein aggregation: folding aggregates, inclusion bodies and amyloid. Fold Des 1998, 3:R9–R23
40. Kopito RR: Aggresomes, inclusion bodies and protein aggregation. Trends Cell Biol 2000, 10:524–530
41. Ross CA, Poirier MA: Protein aggregation and neurodegenerative disease. Nat Med 2004, 10:S10–S17
42. von Nandelstadh P, Soliymani R, Baumann M, Carpen O: Analysis of myotilin turnover provides mechanistic insight into the role of myotilinopathy-causing mutations. Biochem J 2011, 436:113–121
43. Goldfarb LG, Vicart P, Goebel HH, Dalakas MC: Desmin myopathy. Brain 2004, 127:723–734
44. Vicart P, Caron A, Guicheney P, Li Z, Prévost MC, Faure A, Chateau D, Chapon F, Tomé F, Dupret JM, Paulin D, Fardeau M: A missense mutation in the alphaB-crystallin chaperone gene causes a desmin-related myopathy. Nat Genet 1998, 20:92–95
45. Selcen D, Muntoni F, Burton BK, Pegoraro E, Sewry C, Bite AV, Engel AG: Mutation in BAG3 causes severe dominant childhood muscular dystrophy. Ann Neurol 2009, 65:83–89
46. Sharma S, Mücke N, Katus HA, Herrmann H, Bär H: Disease mutations in the "head" domain of the extra-sarcomeric protein desmin distinctly alter its assembly and network-forming properties. J Mol Med (Berl) 2009, 87:1207–1219
47. Bär H, Kostareva A, Sjöberg G, Sejersen T, Katus HA, Herrmann H: Forced expression of desmin and desmin mutants in cultured cells: impact of myopathic missense mutations in the central coiled-coil domain on network formation. Exp Cell Res 2006, 312:1554–1565
48. Bova MP, Yaron O, Huang Q, Ding L, Haley DA, Stewart PL, Horwitz J: Mutation R120G in alphaB-crystallin, which is linked to a desmin-related myopathy, results in an irregular structure and defective chaperone-like function. Proc Natl Acad Sci USA 1999, 96:6137–6142
49. Mologni L, Moza M, Lalowski MM, Carpén O: Characterization of mouse myotilin and its promoter. Biochem Biophys Res Commun 2005, 329:1001–1009